

COMMUNICATION


 Cite this: *RSC Adv.*, 2016, 6, 33369

 Received 29th January 2016
 Accepted 23rd March 2016

DOI: 10.1039/c6ra02663j

www.rsc.org/advances

2-(3',4'-Dimethoxybenzylidene)tetralone induces anti-breast cancer activity through microtubule stabilization and activation of reactive oxygen species†

 Yashveer Gautam,^{‡a} Sonam Dwivedi,^{‡b} Ankita Srivastava,^a Hamidullah,^b Arjun Singh,^a D. Chanda,^a Jyotsna Singh,^b Smita Rai,^b Rituraj Konwar^{*b} and Arvind S. Negi^{*a}

Breast cancer is a leading cause of women mortality worldwide. Diverse analogues of 2-benzylidene tetralone have been synthesized and evaluated for anti-cancer activity against a panel of cancer cell lines. Among these, compounds **13**, **15** and **19** exhibited potent anti-cancer activity ($IC_{50} = 1-3 \mu M$) against human breast cancer cells, MDA-MB-231 and non-toxic towards non-malignant cell line, HEK-293. Compounds **13**, **15** and **19** significantly stabilized tubulin polymerization and arrested cell cycle progression at G0/G1 phase instead of typical mitotic arrest at G2/M phase as observed in case of tubulin polymerization modulators suggesting induction of mitotic slippage followed by cell death. Further, mechanistic studies revealed that compound **13** induced reactive oxygen species generation and apoptosis in breast cancer cells. Inhibition of ROS by *N*-acetyl-L-cysteine prevented compound **13** induced cytotoxicity. Compound **13** showed potent anti-cancer activity (74–79% tumour reduction) in syngeneic rat mammary tumour model without any adverse side effect. It was well tolerated up to 1000 mg kg⁻¹ dose in acute oral toxicity. The identified lead molecule **13** may further be optimized for better activity.

Introduction

Breast cancer is the most common invasive cancer in female worldwide. It accounts 26% of female cancer cases and causes about 18.2% female cancer deaths. Breast cancer affects one in eight women during their lives. It caused 1.7 million patients and about 0.52 million deaths in 2012.¹ The disease has high complexity of more than 18 sub-types of breast cancer. Among various risk factors for developing breast cancer life style, environmental, genetic and biological are predominant. There are a number of treatments available to tackle this cancer including surgery,

radiation therapy, chemotherapy, hormonal therapy and targeted therapy. Based on responsiveness, breast cancer is subdivided into hormone responsive (ER/PR/Her-2) and hormone non-responsive. In chemotherapy, cytotoxic drugs like paclitaxel, taxotere, doxorubicin *etc.*, and hormone antagonists like tamoxifen, fulvestrant and aromatase inhibitors like anastrozole, letrozole *etc.* are in use.² However, multimodality approach is used to eradicate residual breast cancer cells to prevent recurrence of the disease. Several anti-breast cancer drugs have been developed, but the morbidity and mortality of the disease is so high that it is still a challenge to scientific fraternity. Microtubules have been considered as one of the most suitable targets for cancer drug development.^{3,4}

The present study describes development of anti-cancer agents through microtubule modulation. Microtubules are tube like rigid hollow cylindrical filamentous structures built by polymerisation of tubulin dimers.⁵ Microtubules serve as cytoskeletons of the cells and also form framework for structures like spindle apparatus that helps in chromosome segregation during cell division. Owing to their crucial role in mitotic process, microtubules have become an attractive target especially in the treatment of cancer.⁶

We designed 2-substituted 1-tetralone derivatives as possible antitubulins. The basis of designing was inspired from structure–activity relationship of combretastatin A4, a natural antitubulin isolated from African Willow tree *i.e.* *Combretum cefrum*.⁷ According to its SAR, a diaryl system should be separated through a double bond (restricted rotation) and a 3,4,5-trimethoxyphenyl unit should be present at one of the phenyl ring.⁸ The 3,4,5-trimethoxyphenyl fragment is an important motif to interact with microtubule and induces antitubulin effect.⁶ Based on these facts we planned to synthesize 2-benzylidene tetralones as possible anti-cancer agent through microtubule modulation.

Results and discussion

Chemistry

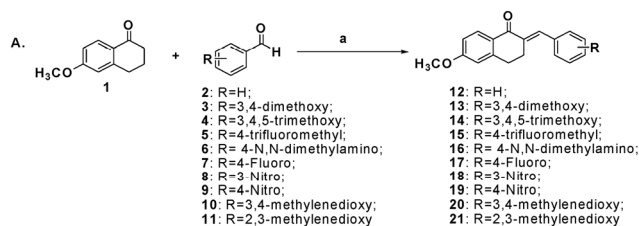
2-Benzylidene tetralones were prepared as per Scheme 1. 6-Methoxytetralone (**1**) was treated with various aromatic benzaldehydes (**2–11**) using 3% alkaline KOH to afford

^aCSIR-Central Institute of Medicinal and Aromatic Plants (CSIR-CIMAP), Kukrail Picnic Spot Road, P.O. CIMAP, Lucknow-226015, India. E-mail: arvindcimap@rediffmail.com

^bCSIR-Central Drug Research Institute (CSIR-CDRI), B.S. 10/1, Sector 10, Jankipuram Extension, Sitapur Road, Lucknow-226031, India. E-mail: r_konwar@cdri.res.in

† Electronic supplementary information (ESI) available: All the ¹H, ¹³C and mass spectra of potential compounds *i.e.* **13**, **15** and **19**. See DOI: 10.1039/c6ra02663j

‡ Equal authorship.



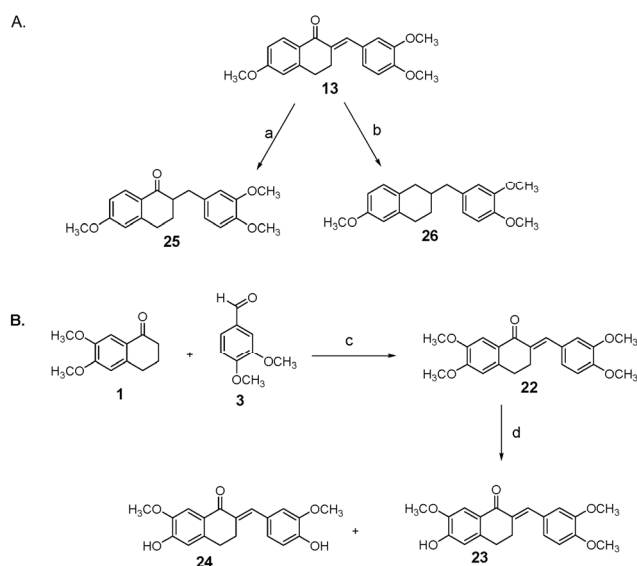
Scheme 1 Reagents and conditions: (a) 3% KOH in MeOH, RT, 2–5 h, 68–86%.

corresponding 2-benzylidenetetralones (**12–21**) in good yields (68–86%) through Claisen–Schmidt reaction. Compounds were purified through column chromatography and confirmed through spectroscopy.

The best analogue of the series *i.e.* compound **13** was further modified as per Scheme 2, to get some structural clues to 2-benzyltetralone (**25**) using catalytic hydrogenation (Pd/C). On reduction with NaBH₄-TFA, compound **13** afforded 2-benzyltetralin (**26**). 6,7-Dimethoxy-2-benzylidene tetralone (**22**) was also prepared as for compounds **12–21**. Compound **22** was selectively demethylated with anhydrous aluminium chloride to get phenolic products **23** and **24**.

Biological evaluation

Cytotoxicity evaluation. All the synthesized compounds were evaluated for anti-cancer activity against breast cancer cell lines MCF-7 (estrogen responsive proliferative breast cancer model) and MDA-MB-231 (estrogen independent aggressive breast cancer model), LA7 (rat mammary tumour), HCT116 (human colon cancer), H1299 (human lung cancer) and non-cancer cell line, HEK-293 (human embryonic kidney) using MTT assay to assess cell inhibition.⁹ Results are shown in Table 1. Out of



Scheme 2 Reagents and conditions: (a) 10% Pd–C, THF, RT, quantitative; (b) NaBH₄-TFA, 0 °C to RT, 53%; (c) 3% KOH in MeOH, RT, 3 h, 79%; (d) AlCl₃-DCM RT, **23** : **24** = 1 : 1, 87%.

fifteen synthesized analogues ten analogues showed significant cytotoxicity (IC₅₀ = 1–47 μM) against MDA-MB-231, LA-7, HCT116 and H1299 cells rest were inactive at 50 μM concentration. However, compounds **13**, **15** and **19** showed potent cytotoxicity (IC₅₀ = 1–3.2 μM) against highly aggressive breast cancer cell line (MDA-MB-231 cells). Compounds **15** effectively inhibited growth of MCF-7, MDA-MB-231, HCT116 and HCT1299 cells. Compound **25** was selective to both breast cancer cell lines. However, compounds **13** and **19** more effectively inhibited MDA-MB-231 cells as compared to other cell lines. Among the entire compounds screened, compound **13** was the most active analogue in this series with lowest IC₅₀ (1.0 μM) against MDA-MB-231 cells and IC₅₀ (7 μM) against LA-7 cells. Furthermore, compound **13** did not show cytotoxicity against non-malignant cells (HEK-293). Collectively, these cytotoxicity data suggest that compound **13** was the most potent against MDA-MB-231 and LA-7 cells.

Structure activity relationship

These analogues had structural diversity mainly at benzylidene ring. However, some definite trends were observed. These compounds mostly exhibited potent cytotoxicity against MDA-MB-231 *i.e.* hormone independent breast cancer cell line. Hence, for SAR we focused on trend against this cell line. Analogue **12** possessing no substitution in benzylidene ring showed marginal activity (IC₅₀ = 40 μM) against MDA-MB-231 cells. While, compound **13** with 3,4-dimethoxy substitution at benzylidene ring was the best analogue (IC₅₀ = 1 μM). But, on introducing another methoxy group at C5' position of benzylidene ring (analogue **14**) activity (IC₅₀ = 42 μM) was reduced drastically as compared to **12**. Introducing a nitro (withdrawing) group at *meta* position (analogue **18**), activity was slightly enhanced (IC₅₀ = 36 μM) but changing the position of nitro group from *meta* to *para* (analogue **19**) activity (IC₅₀ = 1.5 μM) was enhanced remarkably. Similarly, another withdrawing group trifluoromethyl at benzylidene ring (analogue **15**) also exhibited potent cytotoxicity (IC₅₀ = 3.2 μM). But, in case of *p*-fluoro substitution (analogue **17**) activity was abolished.

Analogues **13** exhibited best activity (IC₅₀ = 1.0 μM). On introducing another methoxy group at C7 (analogue **22**) activity was reduced. Partial reduction of analogue **13** to 2-benzyl derivative (**25**), retained potential cytotoxicity (IC₅₀ = 8.9 μM). While reducing the C1-ketone, to C1-methylene (tetralin **26**) compound was inactive. Overall, from these modifications, it may be concluded that C1 ketone is essentially required in the tetralone skeleton and presence of 3,4-dimethoxy in benzylidene ring enhances the cytotoxicity.

Antimitotic activity

Microtubule dynamics is a crucial aspect of mitosis phase in cell cycle. Microtubule interfering agents induce mitotic arrest which leads to increase in 4 N cells at G2/M phase.⁶ Therefore, we examined cell cycle phase distribution of MDA-MB-231 cells followed by compounds **13**, **15** and **19** treatments in MDA-MB-231 cells by PI staining using flow cytometry.¹⁰ In the kinetics graph (Fig. 1), compounds **13**, **15** and **19** showed interference in

Table 1 Cell inhibiting activity of the compounds (IC₅₀ ± SEM in μM)

Comp	MCF-7		MDA-MB-231		LA-7		PC-3		HeLa		Ishikawa		HCT116		H1299		U937		HEK-293		
	24 h	48 h	24 h	48 h	24 h	48 h	24 h	48 h	24 h	48 h	24 h	48 h	24 h	48 h	24 h	48 h	24 h	48 h	24 h	48 h	
12	>50	>50	40 ± 0.01	>50	ND ^a	ND	>50	ND	ND	ND	ND	ND	ND	ND	ND	ND	ND	ND	>50	>50	
13	>50	>50	>50	1 ± 0.01	>50	7 ± 0.03	>50	25 ± 0.05	>50	18 ± 0.03	>50	34 ± 0.01	6.12 ± 0.04	>50	7.5 ± 0.02	19 ± 0.01	>50	>50	>50	>50	
14	>50	>50	>50	>50	ND	ND	>50	ND	ND	ND	ND	ND	ND	ND	ND	ND	ND	ND	>50	>50	
15	>50	12.5 ± 0.01	>50	3.25 ± 0.01	>50	15 ± 0.02	>50	29 ± 0.02	>50	20 ± 0.05	>50	40 ± 0.02	9.76 ± 0.02	>50	10.2 ± 0.01	22 ± 0.03	>50	>50	>50	>50	
18	>50	>50	36.2 ± 0.02	>50	ND	ND	>50	ND	ND	ND	ND	ND	ND	ND	ND	ND	ND	ND	>50	>50	
19	>50	>50	>50	1.53 ± 0.01	>50	18 ± 0.01	>50	30 ± 0.03	>50	25 ± 0.02	>50	42 ± 0.02	22.4 ± 0.07	>50	15.3 ± 0.03	25 ± 0.05	>50	>50	>50	>50	
20	21.6 ± 0.02	>50	>50	>50	ND	ND	>50	ND	ND	ND	ND	ND	ND	ND	ND	ND	ND	ND	>50	>50	
21	>50	>50	>50	>50	ND	ND	>50	ND	ND	ND	ND	ND	ND	ND	ND	ND	ND	ND	>50	>50	
22	>50	>50	43.51 ± 0.02	>50	ND	ND	>50	ND	ND	ND	ND	ND	ND	ND	ND	ND	ND	ND	>50	>50	
25	25.9 ± 0.02	12.6 ± 0.03	>50	8.91 ± 0.01	ND	ND	>50	ND	ND	ND	ND	ND	ND	ND	ND	ND	ND	ND	>50	35.15 ± 0.02	
Paclitaxel	1 ± 0.01	0.32 ± 0.01	3.6 ± 0.01	0.41 ± 0.01	2.4 ± 0.01	1.2 ± 0.02	1.7 ± 0.04	1.1 ± 0.03	1 ± 0.01	0.65 ± 0.03	5.2 ± 0.04	2.9 ± 0.02	0.4 ± 0.01	0.1 ± 0.02	4 ± 0.01	7.5 ± 0.03	1 ± 0.02	1 ± 0.02	1.5 ± 0.01	25 ± 0.01	18 ± 0.02
Tamoxifen	2.60 ± 0.01	1.5 ± 0.02	10 ± 0.02	6 ± 0.01	20 ± 0.07	11 ± 0.05	>50	>50	40 ± 0.04	31 ± 0.02	32.2 ± 0.03	28.7 ± 0.01	45 ± 0.03	38 ± 0.05	25 ± 0.02	30 ± 0.01	5.7 ± 0.04	8.9 ± 0.03	26 ± 0.01	30 ± 0.03	

^a ND = not determined.

tubulin polymerization. Paclitaxel was taken as a positive control. Results showed that compounds **13**, **15** and **19** stabilized tubulin assembly at indicated concentrations in comparison to control groups. Microtubule assembly is vital for many fundamental cellular processes.¹¹ The conversion of tubulin to microtubule is in dynamic equilibrium which is very much crucial for mitotic process. Any disturbance created in this dynamic equilibrium by the microtubule modulators (stabilizers or inhibitors) induces cell death.^{12,13}

Cell cycle analysis

Flow cytogram results revealed that compounds **13**, **15** and **19** induced G0/G1 cells cycle arrest as compared to untreated

vehicle control cells (Fig. 2), while, there was subsequent decrease of synthetic phase (S-phase) of cells cycle. Usually, microtubule stabilizers like paclitaxel are known to induce G2/M arrest.^{14,15} Following mitotic arrest, cells may have two fates, culminating into apoptosis or go for mitotic exit without proper cell division (mitotic slippage) depending on the inhibitor concentration and check point status. In case of mitotic slippage, aberrant mitosis occurs and cells appear arrested in G1 phase due to pseudo G1 accumulation.¹⁶ Since our microtubule polymerization results clearly showed induction of microtubule stabilization, in view of this we believe that the G1 arrest in cell cycle analysis may suggest mitotic slippage into pseudo G1 followed by cell death.^{17,18} Low concentration of paclitaxel has also

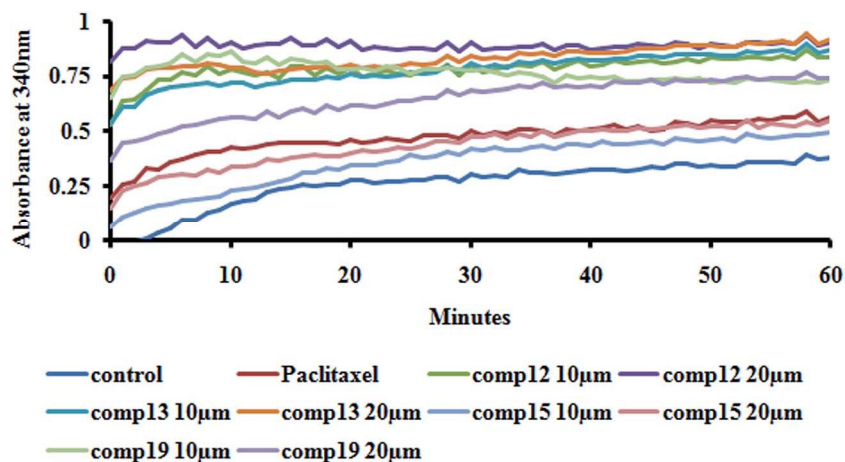


Fig. 1 Tubulin polymerisation kinetics of compounds 12, 13, 15 and 19.

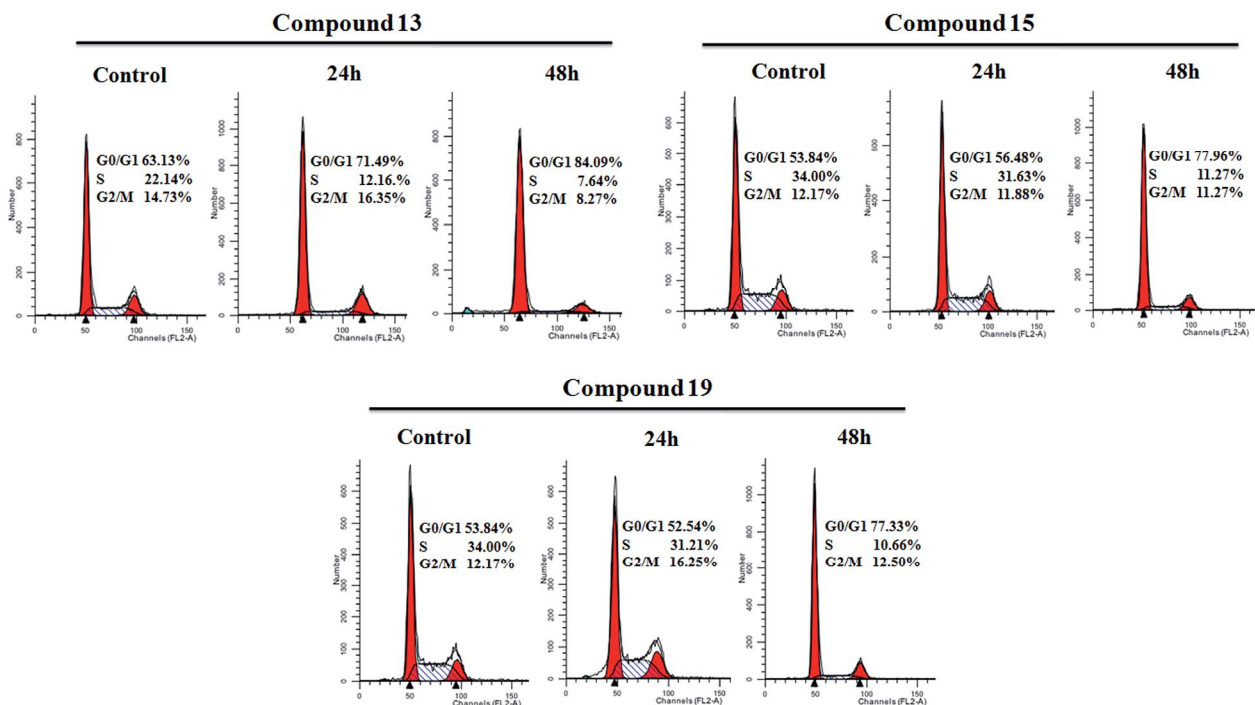


Fig. 2 Effect of compounds **13**, **15** and **19** on cell cycle progression in MDA-MB-231 cells. Cells were treated with compounds **13**, **15** and **19** at 1 μ M for 24 h and 48 h stained with PI and cell cycle was analyzed by flow cytometry.

been showed to induce G1 arrest.^{19,20} In addition, microtubule stabilization and microtubule destabilization leading to mitotic arrest may not be the only processes for inducing anti-tubulin effects. There can be a mixed mechanism which is not fully understood so far, this opens new avenues to explore this area. However, induction of cell cycle arrest in cancer cell lines constitutes one of the most prevalent strategies to stop or limit cancer spreading.^{21,22}

Apoptosis induction

In order to evaluate nuclear morphology in response to compound **13**, Hoechst 33258 staining was carried out using microscopy in MDA-MB-231 cells. Shrunken nucleus and peripherally clumped and fragmented chromatin were seen following compound **13** treatments, a typical characteristic of cells undergone apoptosis (Fig. 3A). To further confirm whether cell growth inhibition was associated with physiological apoptosis or non-specific necrosis AnnexinV-FITC and PI dual staining was carried out using flow cytometer.²³ Compound **13**, the most potent compound of this series induced time dependent increase of apoptotic cells (AnnexinV-FITC stained) and no necrotic (PI stained) population was observed in compound **13** treatment as compare to untreated vehicle control cells (Fig. 3B). Mitotic arrest commonly observed as G2/M arrest

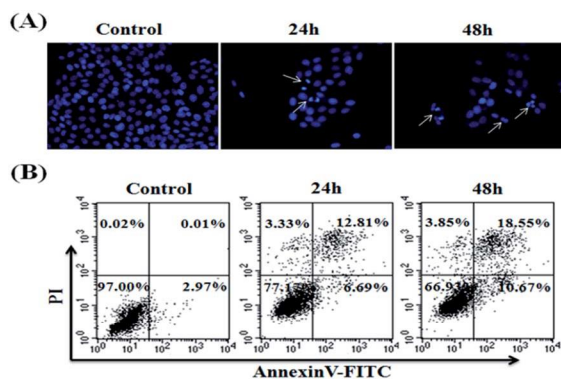


Fig. 3 Effect of compound **13** on nuclear morphology and apoptosis in MDA-MB-231 cells. (A) Cells were treated with compound **13** at $1\ \mu\text{M}$ and nuclear morphology was checked by Hoechst staining by microscopy at $40\times$. (B) Cells were treated with compound **13** at $1\ \mu\text{M}$ for 24 h and 48 h and apoptosis was evaluated using AnnexinV-FITC/PI dual staining kit by flow cytometry.

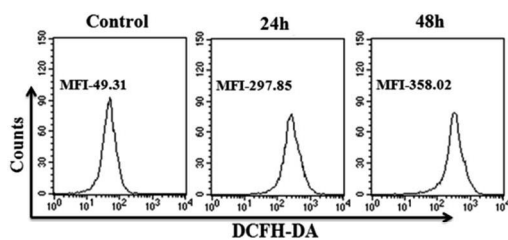


Fig. 4 Effect of compound **13** at $1\ \mu\text{M}$ for 24 h, and 48 h on ROS generation in MDA-MB-231 cells. ROS level was evaluated using DCFH-DA dye by flow cytometry in response to compound **13**.

directly lead to apoptosis called as mitotic death. Here, in our case, treatments of compounds probably induce mitotic slippage which is followed by apoptosis rather than senescence or resistance.

Activation of reactive oxygen species

Effect of compound **13** was evaluated on ROS generation by ROS sensitive probe DCFH-DA staining using flow cytometry in MDA-MB-231 cells.²⁴ There was increased ROS generation detected in compound **13** treated cells as compare to untreated vehicle control cells (Fig. 4). Thus, ROS play as a key mediator in compound **13** mediated apoptosis induction and cancer cell inhibition. Activation of ROS by compound **13** and subsequent apoptosis induction demonstrates a possible pathway leading to cell death by these compounds. Role of ROS in regulation of apoptosis is well accepted and widely documented.^{25,26} Activated of ROS in response to paclitaxel and other microtubule stabilizer is also documented to be associated with apoptosis in cancer cells.²⁷ Therefore, interference in tubulin polymerization induced by compound **13** and subsequent apoptosis is probably mediated by ROS.

To decipher role of increased ROS generation in compound **13** induced cytotoxicity, MDA-MB-231 cells were treated with NAC, a ROS scavenger followed by compound **13** treatment for 48 h and cytotoxicity was evaluated using MTT assay. Result showed that in presence of ROS scavenger compound **13**-mediated cytotoxicity was abolished (Fig. 5). This clearly suggests that ROS generation have a major role during compound **13**-induced cytotoxicity.

In vivo anti-tumour activity against rat mammary tumour

LA7 induced syngenic Sprague Dawley rat mammary tumour model was used to determine *in vivo* anti-cancer efficacy of compound **13**.²⁴ Daily oral administration of $5\ \text{mg}\ \text{kg}^{-1}$ and $10\ \text{mg}\ \text{kg}^{-1}$ of compound **13** resulted in significant regression of tumour as compared to untreated vehicle control group (Fig. 6). In addition, significant reduction of final tumor weight was also observed in the compound **13** treated group. Haematoxylin and eosin staining of tumor tissue section showed densely growing tumor cells with pleomorphic, hyperchromatic nuclei and low cytoplasmic content in untreated vehicle control tumor section (Fig. 7). Tumor tissue section of the compound **13** treated group showed decreased cellular density with vacuolization and elastosis as compared to untreated vehicle control. The

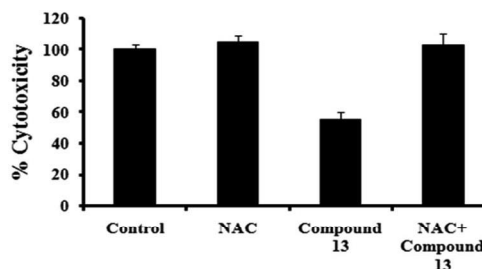


Fig. 5 ROS is required in compound **13**-mediated cytotoxicity in MDA-MB-231 for 48 h.

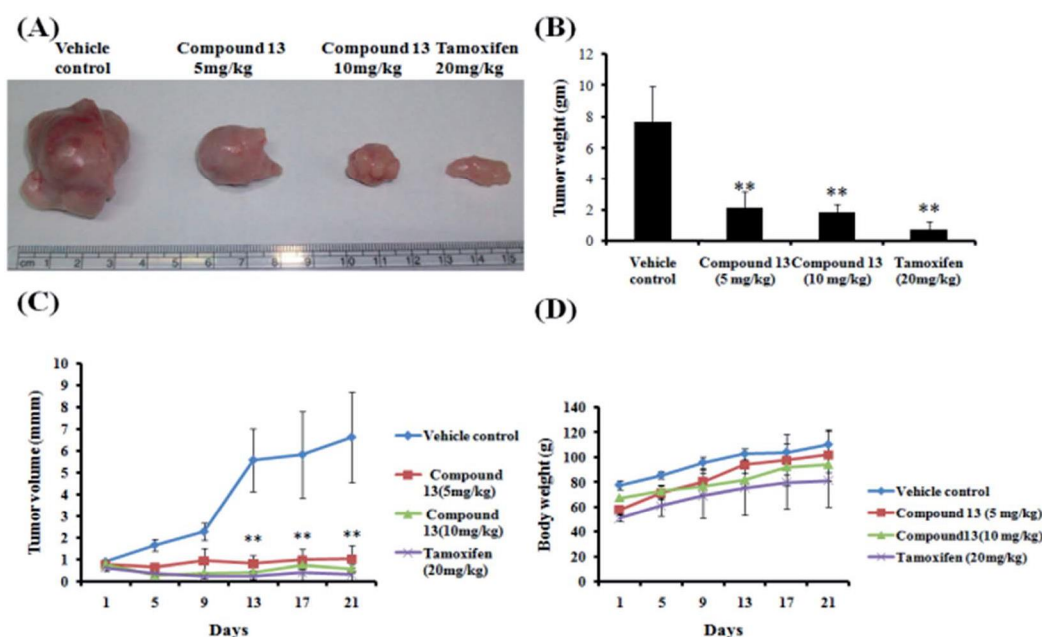


Fig. 6 Effect of compound 13 on tumor regression in syngenic rat mammary tumor model. (A) Compound 13 was daily administered orally and tumor was measured twice a week. At the end, animals were sacrificed, tumors were excised from animals and the tumor was photographed. (B) Tumor volume was calculated and plotted in response to days of treatment. (C) After end of experiment tumor weight was taken and graph was plotted. (D) Body weight was measured twice a week and graph was plotted.

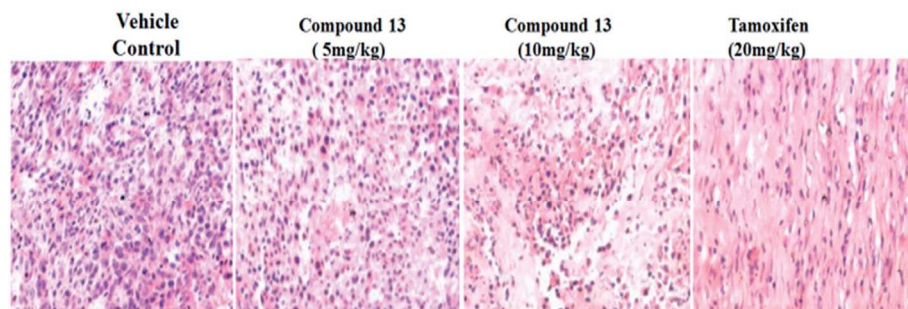


Fig. 7 Histopathology (H & E staining) images of tumor sections of compound 13 tumor tissues shows morphological differences between untreated vehicle control and treated tumor tissues. Magnifications at 20 \times .

histopathological recovery of tumor cellularity was dose dependent. No significant change in terms of body weight was observed in the treated group. Collectively, these *in vivo* results suggest that compound 13 shows potent anti-tumour effect on mammary tumour cells without any apparent cytotoxicity.

In vivo acute oral toxicity

Acute oral toxicity is used to assess the ability of a substance to cause adverse effects within a short period of time following dosing or exposure.²⁸ In acute oral toxicity experiment of compound 13, there were no observational changes, morbidity and mortality throughout the experimental period in all the groups of experimental animals up to the tested dose levels of 1000 mg kg⁻¹. Blood and serum samples upon analysis showed non-significant changes in all the parameters studied like haemoglobin level, RBC count, WBC count, differential leucocytes count, SGPT, ALP, creatinine, triglycerides, cholesterol, albumin,

serum protein (Table 2 & Fig. 8). Animals on gross pathological study showed no changes in any of the organs studied including their absolute and relative weight (Fig. 8). Therefore, the experiment showed that compound 13 was well tolerated by the Swiss albino mice up to the dose level of 1000 mg kg⁻¹ body weight as a single acute oral dose. However, sub-acute and or chronic experiment with the test drug needs to be carried out to look for any adverse effect on repeated exposure to compound 13 in view of significant increase in serum albumin and SGOT level in animals treated with the test drug at 1000 mg kg⁻¹.

Experimental section

General experimental procedures

The starting substrate 6-methoxytetralone was procured from Sigma Chemicals India. Reagents and other chemicals were purchased from Avra Synthesis India and used without purification. Melting points were determined on E-Z Melt automated

Table 2 Effect of compound **13** as a single acute oral dose at 5, 50, 300 and 1000 mg kg⁻¹ on body weight, haematological and serum biochemical parameters in Swiss albino mice (mean ± SE, *n* = 6)

Parameters	Dose of compound 13 at mg kg ⁻¹ body weight as a single oral dose				
	Control	5 mg kg ⁻¹	50 mg kg ⁻¹	300 mg kg ⁻¹	1000 mg kg ⁻¹
Body wt 7 th day (g)	22.43 ± 0.34	23.26 ± 0.69	23.44 ± 0.59	23.03 ± 1.03	23.36 ± 0.76
Haemoglobin (g dL ⁻¹)	13.72 ± 0.79	15.59 ± 1.27	13.41 ± 1.37	14.01 ± 0.33	14.44 ± 0.017
RBC (10 ⁶ /mm ³)	6.53 ± 0.24	6.76 ± 0.19	6.77 ± 0.17	6.78 ± 0.21	7.13 ± 0.25
WBC (1000/mm ³)	10.69 ± 0.80	10.09 ± 0.33	9.75 ± 0.22	9.24 ± 0.32	9.42 ± 0.33
ALP (U L ⁻¹)	297.01 ± 12.10	301.33 ± 18.29	317.73 ± 15.63	298.05 ± 17.44	307.50 ± 20.63
SGPT (U L ⁻¹)	30.34 ± 2.22	30.21 ± 1.82	29.30 ± 2.43	26.68 ± 1.56	29.60 ± 2.15
SGOT (U L ⁻¹)	31.17 ± 1.94	27.71 ± 1.33	26.87 ± 1.04	31.93 ± 2.50	27.27 ± 1.32
Albumin (g dL ⁻¹)	2.15 ± 0.05	1.97 ± 0.11	2.08 ± 0.05	1.97 ± 0.12	2.13 ± 0.10
Creatinine (mg dL ⁻¹)	0.31 ± 0.02	0.43 ± 0.09	0.60 ± 0.06	0.47 ± 0.04	0.63 ± 0.06
Triglycerides (mg dL ⁻¹)	268.94 ± 39.6	245.49 ± 40.9	335.96 ± 23.6	211.03 ± 27.7	303.85.1 ± 29.1
Serum protein (mg mL ⁻¹)	3.09 ± 0.23	2.95 ± 0.29	3.01 ± 0.15	2.96 ± 0.33	3.98 ± 0.30
Cholesterol (mg dL ⁻¹)	219.02 ± 26.6	191.15 ± 28.92	193.68 ± 25.45	205.02 ± 29.93	203.62 ± 25.86

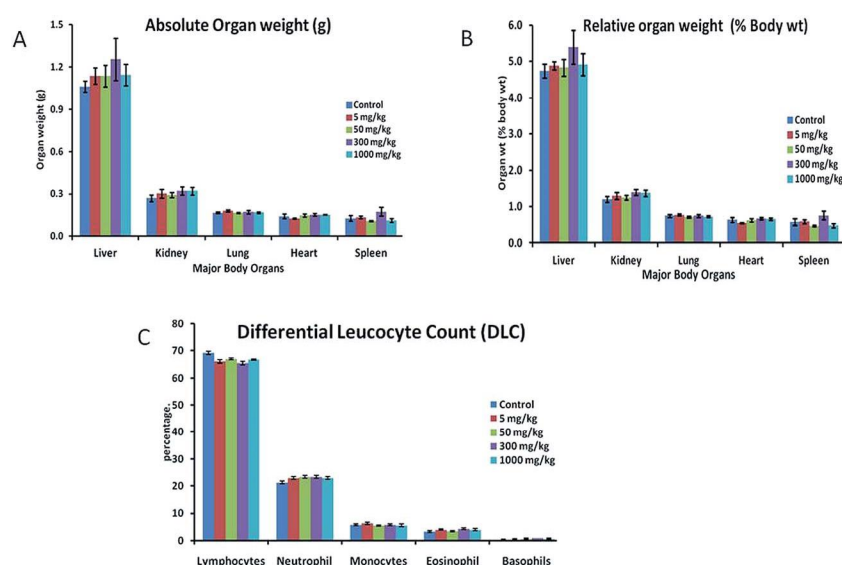


Fig. 8 Effect of compound **13** as a single acute oral dose at 5, 50, 300 and 1000 mg kg⁻¹ on (A) absolute and (B) relative organ weights (C) differential leucocytes counts in Swiss albino mice (*n* = 6, non significant changes were found compared to control).

melting point apparatus in open glass capillaries and were uncorrected. Reactions were monitored on pre-coated silica gel TLC-GF₂₅₄ aluminium sheets (E. Merck, Germany) and visualization was done under UV light (254 nm and 365 nm) and further charring with 2% ceric sulphate in 10% sulphuric acid (aqueous). Compounds were purified through Flash chromatography system (CombiFlash R₂200i, Teledyne-ISCO, USA) using glass columns (13 cm length × 2 cm i.d.) and silica gel (230–400 mesh) using UV detector (254 nm & 280 nm) and characterised by ¹H and ¹³C NMR, ESI-MS, and ESI-HRMS. The purity of the final compound benzylidene indanone **1** was ascertained by reversed phase-HPLC. NMR spectra were obtained on Bruker Avance-DRX300 MHz instrument with tetramethylsilane (TMS) as an internal standard. Chemical shifts are given in δ ppm values. ¹H–¹H coupling constant (*J*) values are given in Hz. ESI mass spectra were recorded on APC3000 LC-MS-MS (Applied Biosystem) and High Resolution Mass (HRMS) on Agilent 6520Q-

TOF after dissolving the compounds in methanol. FT-IR spectra were recorded on Perkin-Elmer Spectrum BX.

DMEM and FBS were purchased from Gibco, India. RNaseA, crystal violet dye, HEPES, trypsin-EDTA, antibiotic-antimycotic (Ab-Am) solution, Phosphate Buffer Saline (PBS), citric acid and propidium iodide (PI) were acquired from Sigma-Aldrich, USA. Sodium bicarbonate (NaHCO₃), agar, sodium citrate and di-sodium hydrogen phosphate were obtained from Himedia Laboratories, India. Solvents including ethanol and isopropanol were procured from Merck, India Ltd. *In vivo* experiments were conducted on Swiss-albino mice after the approval of Institute's Animal Ethical Committee.

Chemical syntheses

General procedure for the synthesis of benzylidene tetralones (12–22). 6-Methoxytetralone (352 mg, 2 mmol) was taken

in 10 mL of 3% potassium hydroxide in methanol (w/v) in an ice-bath (5–10 °C). To this stirred reaction mixture aromatic benzaldehyde (**2-11**, 2 mmol) was added and stirred for 2–5 h. On completion, solvent was evaporated and water (10 mL) was added to it and acidified with 5% dil. HCl (10 mL). The reaction mixture was extracted with ethyl acetate, washed with water and organic layer was dried over anhydrous sodium sulphate. On evaporated, a residue was obtained which was purified through column chromatography over silica gel. On elution with ethyl acetate–hexane the pure product (**12-22**) was obtained in good yield.

2-Benzylidene-6-methoxy-3,4-dihydronaphthalen-1(2H)-one (12). Yield = 83%; mp = 86 °C; ¹H NMR (CDCl₃, 300 MHz): δ 2.89 (bs, 2H, 3-CH₂, *J* = 6.3 Hz), 3.11 (bs, 2H, 4-CH₂, *J* = 5.7 Hz), 3.86 (s, 3H, OCH₃), 6.71 (s, 1H, 5-CH), 6.87 (d, 1H, 7-CH, *J* = 8.7 Hz), 7.26–7.38 (m, 5H, 2-benzylidene phenyl ring), 7.84 (s, 1H, 2-benzylidene CH=), 8.18 (d, 1H, 8-CH, *J* = 8.7 Hz); ¹³C NMR (CDCl₃, 75 MHz): δ 27.63, 29.71, 55.86, 112.70, 113.77, 127.44, 128.30, 129.83, 130.23, 130.55, 131.19, 136.03, 136.44, 146.19, 164.02, 187.26; ESI-MS (MeOH) for C₁₈H₁₆O₂: 265.0 [M + H]⁺, 287.1 [M + Na]⁺, 303.0 [M + K]⁺, 551.2 [2M + Na]⁺.

2-(3',4'-Dimethoxybenzylidene)-6-methoxy-3,4-dihydronaphthalen-1(2H)-one (13). Yield = 86%; mp = 112 °C; ¹H NMR (CDCl₃, 300 MHz): δ 2.91 (bs, 2H, 3-CH₂), 3.21 (bs, 2H, 4-CH₂), 3.85 (s, 3H, OCH₃), 3.90 (s, 6H, 2 × OCH₃), 6.69–8.10 (m, 7H, all aromatic protons and 2-benzylidene CH); ¹³C NMR (CDCl₃, 75 MHz): δ 27.70, 29.60, 55.82, 56.33, 112.64, 112.81, 113.65, 123.54, 127.55, 129.25, 131.06, 134.39, 136.53, 145.93, 149.14, 149.86, 163.89, 187.05; ESI-MS (MeOH) for C₂₀H₂₀O₄: 325 [M + H]⁺, 347 [M + Na]⁺. HRMS (ESI-TOF) *m/z* [M + H]⁺ calcd for C₂₀H₂₁O₄ 325.1440, found 325.1430.

2-(3',4',5'-Trimethoxybenzylidene)-6-methoxy-3,4-dihydronaphthalen-1(2H)-one (14). Yield = 78%; mp = 108 °C; ¹H NMR (CDCl₃, 300 MHz): δ 2.90–2.94 (t, 2H, 3-CH₂, *J* = 6.6 Hz), 3.09–3.14 (t, 2H, 4-CH₂, *J* = 6.2 Hz), 3.85 (s, 3H, OCH₃), 3.88 (s, 3H, OCH₃), 3.89 (s, 3H, OCH₃), 6.66 (bs, 1H, 5-CH), 6.71 (bs, 1H, 7-CH), 6.94 (s, 2H, 2' & 6'-CH of benzylidene ring, *J* = 8.6 Hz), 7.76 (s, 1H, 2-benzylidene CH=), 8.09 (m, 1H, 8-CH); ¹³C NMR (CDCl₃, 75 MHz): δ 27.75, 29.74, 55.83, 56.49, 56.61, 61.22, 107.69, 112.68, 127.42, 128.58, 131.10, 131.90, 136.30, 136.59, 138.96, 146.38, 153.48, 164.00, 188.44; ESI-MS (MeOH) for C₂₁H₂₂O₅: 355 [M + H]⁺; negative mode: 353 [M – H][–].

2-(4'-Trifluoromethylbenzylidene)-6-methoxy-3,4-dihydronaphthalen-1(2H)-one (15). Yield = 70%; mp = 136 °C; ¹H NMR (CDCl₃, 300 MHz): δ 2.38 (bs, 2H, 3-CH₂), 2.51 (bs, 2H, 4-CH₂), 3.33 (s, 3H, OCH₃), 6.16 (s, 1H, 5-CH), 6.36 (d, 1H, 7-CH, *J* = 8.7 Hz), 6.97 (d, 2H, 2' & 6'-CH of benzylidene ring, *J* = 8.6 Hz), 7.11 (d, 2H, 3' & 5'-CH of benzylidene ring); 7.26 (s, 1H, 2-benzylidene CH=), 7.58 (d, 1H, 8-CH, *J* = 8.7 Hz); ¹³C NMR (CDCl₃, 75 MHz): δ 27.60, 29.61, 55.87, 112.76, 113.94, 125.71, 125.76, 127.20, 130.24, 131.29, 134.42, 137.96, 146.10, 164.23, 186.71; ESI-MS (MeOH) for C₁₉H₁₅F₃O₂: 333.3 [M + H]⁺, 355.2 [M + Na]⁺, 371.1 [M + K]⁺.

2-(4'-N,N-Dimethylaminobenzylidene)-6-methoxy-3,4-dihydronaphthalen-1(2H)-one (16). Yield = 68%; mp = 151 °C; ¹H NMR (CDCl₃, 300 MHz): δ 2.90 (t, 2H, 3-CH₂, *J* = 6.2 Hz), 3.01 (s, 6H,

N-(CH₃)₂), 3.13 (bs, 2H, 4-CH₂), 3.86 (s, 3H, OCH₃), 6.69 (bs, 3H, 5-CH and 2' & 6'-CH of 2-benzylidene ring), 6.86 (d, 1H, 7-CH, *J* = 8.7 Hz), 7.41 (d, 2H, 3' & 5'-CH of benzylidene ring, *J* = 8.4 Hz), 7.81 (s, 1H, 2-benzylidene CH=), 8.10 (d, 1H, 8-CH, *J* = 8.7 Hz); ¹³C NMR (CDCl₃, 75 MHz): δ 27.79, 29.62, 30.11, 40.61, 55.81, 112.10, 112.56, 113.44, 124.26, 127.93, 130.93, 131.73, 132.33, 137.57, 145.81, 150.86, 163.62, 187.21; ESI-MS (MeOH) for C₂₀H₂₁NO₂: 308.2 [M + H]⁺, 330.2 [M + Na]⁺, 346.0 [M + K]⁺.

2-(4'-Fluorobenzylidene)-6-methoxy-3,4-dihydronaphthalen-1(2H)-one (17). Yield = 82%; mp = 105 °C; ¹H NMR (CDCl₃, 300 MHz): δ 2.84 (bs, 2H, 3-CH₂), 2.98 (bs, 2H, 4-CH₂), 3.79 (s, 3H, OCH₃), 6.62 (s, 1H, 5-CH), 6.78 (d, 1H, 7-CH, *J* = 8.4 Hz), 7.14–7.17 (d, 2H, 2' & 6'-CH of benzylidene ring, *J* = 8.7 Hz), 7.79 (s, 1H, 2-benzylidene CH=), 8.09 (d, 1H, 8-CH, *J* = 8.9 Hz), 8.2 (d, 2H, 3' & 5'-CH of benzylidene ring); ¹³C NMR (CDCl₃, 75 MHz): δ 27.55, 29.61, 55.85, 112.70, 113.79, 115.75, 116.04, 127.37, 131.18, 132.00, 132.11, 132.52, 135.22, 135.82, 146.02, 161.28, 164.06, 164.58, 186.97; ESI-MS (MeOH) for C₁₈H₁₅FO₂: 283.3 [M + H]⁺, 305.3 [M + Na]⁺, 565.6 [2M + H]⁺.

2-(3'-Nitrobenzylidene)-6-methoxy-3,4-dihydronaphthalen-1(2H)-one (18). Yield = 73%; mp = 163 °C; ¹H NMR (CDCl₃, 300 MHz): δ 2.92 (t, 2H, 3-CH₂, *J* = 6.2 Hz), 3.06 (t, 2H, 4-CH₂, *J* = 5.9 Hz), 3.85 (s, 3H, OCH₃), 6.69 (s, 1H, 5-CH), 6.85 (d, 1H, 7-CH, *J* = 8.7 Hz), 7.57 (t, 1H, CH of 3'-CH of benzylidene ring, *J* = 8.0 Hz), 7.68 (d, 1H, 2'-CH benzylidene ring, *J* = 7.5 Hz); 7.78 (s, 1H, 2-benzylidene CH=), 8.08 (d, 1H, 8-CH, *J* = 8.7 Hz), 8.16 (d, 1H, 4'-CH of benzylidene ring), 8.26 (s, 1H, 6'-CH of benzylidene ring); ¹³C NMR (CDCl₃, 75 MHz): δ 27.56, 29.48, 55.90, 112.76, 114.05, 123.29, 124.46, 127.05, 131.32, 133.21, 136.03, 138.12, 138.50, 146.03, 148.72, 164.32, 186.37; ESI-MS (MeOH) for C₁₈H₁₅NO₄: 310 [M + H]⁺, 332 [M + Na]⁺.

2-(4'-Nitrobenzylidene)-6-methoxy-3,4-dihydronaphthalen-1(2H)-one (19). Yield = 71%; mp = 187 °C; ¹H NMR (CDCl₃, 300 MHz): δ 2.73 (dt, 2H, 3-CH₂, *J* = 6.3), 2.93 (t, 2H, 4-CH₂, *J* = 5.9 Hz), 3.87 (s, 3H, OCH₃), 6.60 (s, 1H, 5-CH), 6.88 (d, 1H, 7-CH, *J* = 8.4 Hz), 7.14–7.17 (d, 2H, 2' & 6'-CH of benzylidene ring, *J* = 8.7 Hz), 7.79 (s, 1H, 2-benzylidene CH=), 8.09 (d, 1H, 8-CH, *J* = 8.9 Hz), 8.2 (d, 2H, 3' & 5'-CH of benzylidene ring); ¹³C NMR (CDCl₃, 75 MHz): δ 27.71, 29.49, 55.91, 112.79, 114.07, 124.06, 124.06, 127.01, 130.74, 130.74, 131.34, 133.36, 139.18, 143.14, 146.06, 147.59, 164.36, 186.32; ESI-MS (MeOH) for C₁₈H₁₅NO₄: 310.3 [M + H]⁺, 332.3 [M + Na]⁺, 348.1 [M + K]⁺, 619.5 [2M + H]⁺, 641 [2M + Na]⁺, 657.4 [2M + K]⁺.

2-(3',4'-Methylenedioxybenzylidene)-6-methoxy-3,4-dihydronaphthalen-1(2H)-one (20). Yield = 82%; mp = 173 °C; ¹H NMR (CDCl₃, 300 MHz): δ 2.92 (t, 2H, 3-CH₂, *J* = 6.3 Hz), 3.10 (t, 2H, 4-CH₂, *J* = 5.9 Hz), 3.87 (s, 3H, OCH₃), 6.01 (s, 2H, O-CH₂-O), 6.72 (s, 1H, 5-CH), 6.86–6.97 (m, 4H, 4 × CH, aromatic), 7.73 (s, 1H, 2-CH of benzylidene); 8.07 (d, 1H, 8-CH, *J* = 8.7 Hz); ESI-MS (MeOH) for C₁₉H₁₆O₄: 309.3 [M + H]⁺, 331.3 [M + Na]⁺, 347.1 [M + K]⁺.

2-(2',3'-Methylenedioxybenzylidene)-6-methoxy-3,4-dihydronaphthalen-1(2H)-one (21). Yield = 86%; mp = 101 °C; ¹H NMR (CDCl₃, 300 MHz): δ 2.47 (bs, 2H, 3-CH₂), 2.54 (bs, 2H, 4-CH₂), 3.41 (s, 3H, OCH₃), 5.54 (s, 2H, O-CH₂-O), 6.23 (s, 1H, 5-CH), 6.23–6.41 (bs, 4H, CH, aromatic), 7.26 (s, 1H, CH of benzylidene ring, *J* = 8.6 Hz), 7.67 (bs, 1H, CH aromatic); ¹³C NMR (CDCl₃,

75 MHz): δ 28.24, 29.71, 55.84, 101.35, 108.96, 112.72, 113.72, 118.84, 121.77, 122.97, 127.40, 129.48, 131.17, 137.64, 146.44, 148.03, 163.99, 186.69; ESI-MS (MeOH) for $C_{19}H_{16}O_4$: 309 $[M + H]^+$.

2-(3',4'-Dimethoxybenzylidene)-6,7-dimethoxy-3,4-dihydronaphthalen-1(2H)-one (22). Yield = 79%; mp = 345 °C (blackens); 1H NMR ($CDCl_3$, 300 MHz): δ 2.89 (t, 2H, 3- CH_2 , J = 6.3 Hz), 3.14 (t, 2H, 4- CH_2 , J = 5.9 Hz), 3.91 (s, 12H, 4 \times OCH_3), 6.66 (s, 1H, =CH of benzylidene), 6.88 (d, 1H, 3'-CH of benzylidene phenyl, J = 8.4 Hz), 6.97 (s, 1H, CH, aromatic), 7.04 (d, 1H, 2'-CH of benzylidene phenyl, J = 8.4 Hz), 7.62 (s, 1H, 5-CH), 7.77 (s, 1H, 8-CH); ^{13}C NMR ($CDCl_3$, 75 MHz): δ 27.93, 28.97, 56.35, 56.47, 110.12, 110.28, 111.39, 123.49, 127.14, 129.30, 134.25, 136.50, 138.39, 148.67, 149.18, 149.87, 153.87, 187.03; ESI-MS (MeOH) for $C_{21}H_{22}O_5$: 354 $[M + H]^+$.

Synthesis of 23 and 24

Compound 22 (200 mg, 0.56 mmol) was taken in dry DCM (10 mL). To this stirred solution anhydrous aluminium chloride (200 g, 1.5 mmol) was added and further stirred for 20 minutes to get products 23 and 24 in 3 : 1.

2-(3',4'-Dimethoxybenzylidene)-6-hydroxy-7-methoxy-3,4-dihydronaphthalen-1(2H)-one (23). Yield = 108 mg (56%); mp = 149 °C; 1H NMR ($CDCl_3$, 300 MHz): δ 2.89 (t, 2H, 3- CH_2), 3.15 (t, 2H, 4- CH_2), 3.91 (s, 3H, OCH_3), 3.94 (s, 6H, 2 \times OCH_3), 3.96 (s, 3H, OCH_3), 6.67 (s, 1H, CH of benzylidene ring), 6.97–6.98 (m, 3H, CH aromatic of benzylidene phenyl ring), 7.63 (s, 1H, 5-CH), 7.78 (s, 1H, 8-CH); ^{13}C NMR ($CDCl_3$, 75 MHz): δ 28.24, 29.71, 55.84, 101.35, 108.96, 112.72, 113.72, 118.84, 121.77, 122.97, 127.40, 129.48, 131.17, 137.64, 146.44, 148.03, 163.99, 186.69; ESI-MS (MeOH) for $C_{19}H_{18}O_4$: 341 $[M + H]^+$.

2-(3'-Methoxy-4'-hydroxybenzylidene)-6-hydroxy-7-methoxy-3,4-dihydronaphthalen-1(2H)-one (24). Compound 22 (200 mg, 0.56 mmol) was taken in dry DCM (10 mL). To get compound 24 in higher quantity, aluminium chloride (600 mg, 4.5 mmol) is added and reaction time is for an hour to get 23 : 24 in 1 : 5.

Yield = 134 mg (73%); mp = 167 °C; 1H NMR ($CDCl_3$, 300 MHz): δ 2.88 (bs, 2H, 3- CH_2), 3.14 (bs, 2H, 4- CH_2), 3.91 (s, 3H, OCH_3), 3.95 (s, 3H, OCH_3), 6.78 (s, 1H, =CH of benzylidene), 6.89–6.97 (m, 3H, aromatic), 7.65 (s, 1H, 5-CH), 7.76 (s, 1H, 8-CH); ^{13}C NMR ($CDCl_3$, 75 MHz): δ 27.90, 28.71, 56.39, 56.62, 109.99, 113.11, 114.83, 116.17, 124.09, 126.99, 134.08, 136.73, 139.15, 146.30, 146.64, 146.78, 150.96, 188.00; ESI-MS (MeOH) for $C_{19}H_{16}O_5$: 327.3 $[M + H]^+$, 349.2 $[M + Na]^+$, 365.2 $[M + K]^+$.

2-(3',4'-Dimethoxybenzyl)-6-methoxy-3,4-dihydronaphthalen-1(2H)-one (25). Benzylidene tetralone 13 (200 mg, 0.62 mmol) was taken in dry THF (10 mL). To this stirred solution Pd-C (10%, 100 mg) was added. Hydrogen gas was supplied through balloon at room temperature. The reaction was stirred for an hour. On completion the reaction mixture was filtered through celite bed, washed with ethyl acetate and evaporated. The residue thus obtained was recrystallised with chloroform–hexane (1 : 3) to get 25 as amorphous solid.

Yield = 179 mg (89%); mp = 99 °C; 1H NMR ($CDCl_3$, 300 MHz): δ 1.43 (bs, 2H, CH_2 , benzylic), 2.02 (bs, 1H, 2-CH), 2.90 (bs, 2H, 3- CH_2), 3.14 (bs, 2H, 4- CH_2), 3.94 (bs, 9H, 3 \times OCH_3),

6.68 (s, 2H, CH_2 of benzylic), 6.77–7.11 (m, 3H, aromatic), 7.77 (s, 1H, 5-CH), 8.09 (s, 1H, 8-CH); ^{13}C NMR ($CDCl_3$, 75 MHz): δ 27.70, 29.75, 30.09, 55.80, 56.31 \times 2, 111.33, 112.63, 113.64, 123.55, 127.52, 129.23, 131.06, 134.35, 136.57, 145.93, 149.12, 149.86, 163.89, 187.06; ESI-MS (MeOH) for $C_{20}H_{22}O_4$: 327 $[M + H]^+$.

2-(3',4'-Dimethoxybenzyl)-6-methoxy-1,2,3,4-tetrahydronaphthalen (26). To a stirred solution of benzylidene tetralone 13 (200 mg, 0.62 mmol) in TFA (1 mL) at 5–10 °C, sodium borohydride (150 mg, 4 mmol) was added in portions over a period of 20 min and further stirred for an hour. On completion the reaction mixture was poured to crushed ice and extracted with ethyl acetate (15 mL \times 2), washed with water and dried over anhydrous sodium sulphate. The dried organic layer was evaporated *in vacuo* and crude mass was purified through column chromatography over silica gel (100–200 mesh) to get pure 26.

Yield = 102 mg (53%); mp = 74 °C; 1H NMR ($CDCl_3$, 300 MHz): δ 1.49 (bs, 2H, CH_2 , benzylic), 2.00 (m, 1H, 2-CH), 2.62 (bs, 2H, 3- CH_2), 2.79 (bs, 2H, 4- CH_2), 3.76 (s, 3H, OCH_3), 3.88 (s, 6H, 2 \times OCH_3), 6.66–6.96 (m, 6H, CH, aromatic); ^{13}C NMR ($CDCl_3$, 75 MHz): δ 29.50, 29.78, 35.54, 37.00, 42.85, 55.64, 56.25, 56.32, 111.50, 112.27, 112.75, 113.83, 121.43, 129.07, 130.36, 133.85, 138.17, 147.64, 149.16, 157.92; ESI-MS (MeOH) for $C_{20}H_{24}O_3$: 313 $[M + H]^+$, 335 $[M + Na]^+$, 351 $[M + K]^+$.

Biological assays

Cell cultures. Human breast cancer cell lines MCF-7 (ER+ve) and MDA-MB-231 (ER–ve), LA-7 (rat mammary tumour), PC-3 (human prostate cancer), HeLa (human cervical cancer), Ishikawa (human endometrial cancer), HCT116 (human colorectal cancer), H1299 (human small non-small lung cancer) and U935 (human histiocytic lymphoma), were originally obtained from American type of cell culture collection (ATCC) and human embryonic kidney cell (HEK-293) were obtained from Institute's cell repository of animal tissue culture facility (CSIR-CDRI, Lucknow). Cells were cultured in DMEM (Dulbecco modified eagle medium, Sigma) supplemented with 10% FBS (GIBCO BRL Laboratories, New York, USA) and 1% antibiotic-antimycotic solution (Sigma Chemical CO., St Louis, MO, USA) at 37 °C with 5% CO_2 in humidified chamber. LA7 cells were cultured in DMEM supplemented with 5%FBS, 5 μ g mL^{-1} insulin and 50 nM hydrocortisone and HCT116 was cultured in McCoy's 5A media supplemented with 10% FBS.

In vitro cell proliferation assay. The anti-cancer activity of tetralone derivatives was determined using 3-(4,5-dimethylthiazol-2-yl)-2,5-diphenyltetrazoliumbromide (MTT) assay as described earlier.⁹ Briefly, cells (1×10^4 cells) were seeded in 96-well microculture plates in 200 μ L DMEM for 24 h. Compounds were diluted to desired concentrations in culture medium DMEM without phenol red free DMEM culture medium and incubated for 24 h and 48 h. In case of inhibitor study, cells were pre-treated with 10 mM NAC for 2 h followed by compound 13 for 48 h. At the end of incubation, 20 μ L of 5 mg mL^{-1} was added to each well and the plates were further incubated for 3 h. Thereafter, supernatant from each well was carefully removed and formazan crystals were dissolved in 200

μL of dimethylsulphoxide (DMSO) using plate shaker (Biosan) and absorbance was recorded in a microplate reader at 570 nm wavelength (Microquant; BioTek).

Cell cycle analysis. Cell cycle analysis was carried out to check distribution of the cells in different phases induced by compound **13**, **15** and **19** using propidium iodide (PI) staining method. MDA-MB-231 cells (1×10^6 cells) were seeded in T-25 culture flask and allowed to grow for 24 h. After 24 h, cells were treated with compound **13** for 24 h and 48 h. At end of incubation, cells were harvested, fixed in ice cold 70% ethanol and incubated for 1 h at 4 °C. Thereafter, cells were centrifuged and resuspended in 300 μL PBS and incubated with 30 μg of RNaseA and 15 μg of PI for 30 minutes at room temperature in dark. Samples were analyzed by flow cytometry using FACSCalibur instrument (BD biosciences).

Apoptosis analysis. To determine effect of compound **13** on apoptosis in MDA-MB-231 cells, AnnexinV-FITC/PI dual staining was carried out by flow cytometry.²⁴ Cells (1×10^6 cells) were seeded in six well plates and allowed to grow for 24 h. Cells were treated with compound **13** for 24 h and 48 h. At the end of incubation cells were harvested, washed with PBS and stained with AnnexinV-FITC and PI using apoptosis detection kit (sigma). Samples were acquired by flow cytometer using FACSCalibur instrument (BD biosciences).

ROS generation assay. ROS generation was measured using 2,7-dichlorodihydrofluorescein diacetate dye by flow cytometer.²⁴ MDA-MB-231 cells (1×10^6) were seeded in 6 well plates for 24 h. Cells were treated with compound **13** for 24 h and 48 h. At the end of incubation, cells were harvested by trypsinization, fixed in cold methanol and incubated with 30 $\mu\text{g mL}^{-1}$ of DCFH-DA dye for 30 minutes in dark at room temperature. After the end of incubation, cells were centrifuged, resuspended in 300 μL of PBS. Samples were analyzed by flow cytometry using FACSCalibur instrument (BD biosciences).

Hoechst staining. Nuclear fragmentation was detected by staining nuclei with Hoechst 33258. MDA-MB-231 cells (1×10^6) were seeded in six well plates for 24 h. Thereafter, cells were treated with compound **13** for 24 h and 48 h. Cells were washed with PBS and fixed with 4% paraformaldehyde and permeabilized with 0.5% TritonX-100. Cells were stained with Hoechst 33258 and images were captured using fluorescence microscope (Leica).

Tubulin polymerisation assay. Tubulin polymerization experiment was done as per reported method using 'assay kit' from Cytoskeleton, USA.^{5,11} In brief, tubulin protein (3 mg mL^{-1}) in tubulin polymerization buffer (80 mM PIPES, pH 6.9, 2 mM MgCl_2 , 0.5 mM EGTA, 1 mM GTP and 15% glycerol) was placed in pre-warmed 96-well microtiter plates at 37 °C in the presence of test compounds with variable concentrations. All samples were mixed well and polymerization was monitored kinetically at 340 nm every min for 1 h using Spectramax plate reader. Paclitaxel (taxol) was used as standard stabilizer of tubulin polymerisation.

In vivo tumor regression. Animal studies were coordinated by prior approval from the Institutional Animal Ethics committee (IAEC), CSIR-CDRI, Lucknow. Adult Sprague Dawley (SD) rat were used to develop syngenic mammary tumor model.²⁴ Briefly,

LA-7 (6×10^6) cells were inoculated into mammary fat pad of female SD rats. After one week, when tumor size were measurable, animals were randomly grouped. 5 mg kg^{-1} and 10 mg kg^{-1} body weight of compound **13** was orally administered daily. Control group receive vehicle only. During this period, tumors size were measured twice a week and tumor volume was calculated using formula; $V = [(\text{length}) \times (\text{width})^2]/2$.

Hematoxylin and eosin (H & E) staining. Formalin-fixed tumor tissue was used for histopathological studies. After deparaffinization and dehydration, tissue samples were stained with Harris-hematoxylin and eosin stains. The images were taken under 20 \times magnification using light microscopy (OlympusBX51, Tokyo, Japan). For each group, sections from at least three rats ($n = 3$) were examined for histopathological analysis.

Acute oral toxicity. In view of potent anti-cancer activity of compound **13**, acute oral toxicity of the same was carried out in Swiss albino mice for its further development as a drug candidate. Experiment was conducted in accordance with the Organization for Economic Co-operation and Development (OECD) test guideline no 423 (1987). Briefly, 30 mice (15 male and 15 female) were taken and divided into four groups comprising 3 male and 3 female mice in each group weighing between 20 and 25 g. The animals were maintained at 22 ± 5 °C with humidity control and also on an automatic dark and light cycle of 12 hours. The animals were fed with the standard mice feed and provided *ad libitum* drinking water. Mice of group 1 (Group I) were kept as control and animals of groups 2, 3, 4 and 5 (Groups II, III, IV & V) were kept as experimental. The animals were acclimatized for 7 days in the experimental environment prior to the actual experimentation. Compound **13** was dissolved in minimum volume of DMSO, diluted with 0.7% CMC (carboxymethylcellulose) and was given at 5, 50, 300 and 1000 mg kg^{-1} body weight to animals of groups 2, 3, 4 and 5 (Groups II, III, IV & V) respectively once orally. Control animals received only vehicle. The animals were checked for mortality and any signs of ill health at hourly interval on the day of administration of drug and there after a daily general case side clinical examination was carried out for changes in skin, mucous membrane, eyes, occurrence of secretion and excretion and also responses like lachrymation, pilo-erection respiratory patterns *etc.* Also changes in gait, posture and response to handling were also recorded.²⁹ In addition to observational study, body weights were recorded and blood and serum samples were collected from all the animals on 7th day of the experiment in acute oral toxicity. The samples were analyzed for total RBC, WBC, differential leucocytes count, haemoglobin percentage and biochemical parameters like ALP, SGPT, SGOT, total cholesterol, triglycerides, creatinine, bilirubin, serum protein and tissue protein activity. The animals were then sacrificed and were necropsed for any gross pathological changes. Weights of vital organs like liver, heart, kidney *etc.* were recorded.³⁰

Statistical analysis. Data were expressed as means \pm SEM. The statistical significance between values of treated samples and controls were determined by one-way ANOVA using GraphPad Prism version 3.0.

Conclusions

In conclusion, 2-benzylidene tetralones have been explored as potent anti-breast cancer agents. The representative compounds **13** and **19** exhibited potent anti-breast cancer activity. The most active compound of this series, compound **13** induced stabilization of tubulin polymerization similar to paclitaxel along with cell cycle arrest and apoptosis. However, compound **13** showed G1 arrest unlike other microtubule inhibitors possibly due to mitotic slippage associated secondary apoptosis. Tubulin stabilizers are known to activate ROS and we observed a significant induction of ROS by compound **13**. ROS dependent cell death was further confirmed with inhibition of ROS using its scavenger that abrogated compound induced apoptosis. This suggested that interference in tubulin polymerisation by compound **13** is possibly linked with ROS generation and cancer cell death. Most interestingly, compound **13** reduced rat mammary tumour growth *in vivo* by 74–79% at both 5 mg kg⁻¹ and 10 mg kg⁻¹. The additional data on acute oral toxicity suggested that compound **13** can be well tolerated by the mice up to 1000 mg kg⁻¹ dose without any adverse effects. Compound **13** could serve as promising lead molecule for targeting breast cancer inhibition through tubulin stabilization and microtubule exit without significance *in vitro* and *in vivo* toxicity.

Conflict of interest

The authors declare no competing financial interest.

Acknowledgements

We are grateful to SERB-DST for funding support. Senior Research Fellowship to the authors (YG) and (H) from Council of Scientific and Industrial Research (CSIR) and Department of Biotechnology respectively is duly acknowledged. We also thank Mr AL Vishwakarma, SAIF, CSIR-CDRI for flow cytometric analysis.

References

- 1 WHO, Cancer factsheet No 297, February 2015.
- 2 B. S. Komm and S. Mirkin, *J. Steroid Biochem. Mol. Biol.*, 2014, **143**, 207.
- 3 A. Jordan, J. A. Hadfield, N. J. Lawrence and A. T. McGown, *Med. Res. Rev.*, 1998, **18**, 259.
- 4 M. A. Jordan and L. Wilson, *Nat. Rev. Cancer*, 2004, **4**, 253.
- 5 M. L. Shelanski, F. Gaskin and C. R. Cantor, *Proc. Natl. Acad. Sci. U. S. A.*, 1973, **70**, 765.
- 6 A. S. Negi, Y. Gautam, S. Alam, D. Chanda, S. Luqman, J. Sarkar, F. Khan and R. Konwar, *Bioorg. Med. Chem.*, 2015, **23**, 373.
- 7 G. R. Pettit, G. M. Cragg and S. B. Singh, *J. Nat. Prod.*, 1987, **50**, 386.
- 8 G. C. Tron, T. Piralì, G. Sorba, F. Pagliai, S. Busacca and A. A. Genazzani, *J. Med. Chem.*, 2006, **49**, 3033.
- 9 Hamidullah, R. Kumar, K. S. Saini, A. Kumar, E. Ramakrishna, R. Maurya, R. Konwar and N. Chattopadhyay, *Biochemie*, 2015, **119**, 68.
- 10 C. Riccardi and I. Nicoletti, *Nat. Protoc.*, 2006, **1**, 1458.
- 11 J. C. Lee and S. N. Timasheff, *Biochemistry*, 1977, **16**, 1754.
- 12 D. L. Sacket and R. E. Lippoldt, *Biochemistry*, 1991, **30**, 3511.
- 13 M. K. Gardener, B. D. Charlebois, I. M. Janosi, J. Howard, A. J. Hunt and D. J. Odde, *Cell*, 2011, **146**, 582.
- 14 P. B. Schiff, J. Fant and S. B. Horwitz, *Nature*, 1979, **277**, 665.
- 15 B. A. Weaver, *Perspective on Cell Biology and Human Health*, 2014, vol. 25, p. 2677.
- 16 P. Karna, S. M. Sharp, C. Yates, S. Prakash and R. Aneja, *Mol. Cancer*, 2009, **8**, 93.
- 17 M. V. Blagosklonny, *Cell Cycle*, 2007, **6**, 70.
- 18 K. E. Gascoigne and S. S. Taylor, *J. Cell Sci.*, 2009, **122**, 2579.
- 19 P. Giannakakou, R. Robey, T. Fojo and M. V. Blagosklonny, *Oncogene*, 2001, **20**, 3806.
- 20 Z. N. Demidenko, S. Kalurupalle, C. Hanco, C. U. Lim, E. Broude and M. V. Blagosklonny, *Oncogene*, 2008, **27**, 4402.
- 21 L. H. Hartwell and T. A. Weinert, *Science*, 1989, **246**, 629.
- 22 C. J. Sherr, *Science*, 1996, **274**, 1672.
- 23 S. K. Dwivedi, K. Samanta, M. Yadav, A. K. Jana, A. K. Singh, B. Chakravarti, S. Mondal, R. Konwar, A. K. Trivedi, N. Chattopadhyay, S. Sanyal and G. Panda, *Bioorg. Med. Chem. Lett.*, 2013, **23**, 6816.
- 24 Hamidullah, K. S. Saini, N. Devender, A. Bhattacharjee, S. Das, S. Dwivedi, M. P. Gupt, H. K. Bora, K. Mitra, R. P. Tripathi and R. Konwar, *Int. J. Biochem. Cell Biol.*, 2015, **65**, 275.
- 25 H. U. Simon, A. Haj-Yehia and F. Levi-Schaffer, *Apoptosis*, 2000, **5**, 415.
- 26 D. Trachootham, J. Alexandre and P. Huang, *Nat. Rev. Drug Discovery*, 2009, **8**, 579.
- 27 H. Fawcett, J. S. Mader, M. Robichaud, C. Giacomantonio and D. W. Hoskin, *Int. J. Oncol.*, 2005, **27**, 1717.
- 28 M. N. Ghosh, in *Fundamentals of Experimental Pharmacology*, Scientific Book Agency, Kolkata, 1st edn, 1984, p. 156.
- 29 J. J. Allan, A. Damodaran, N. S. Deshmukh, K. S. Goudar and A. Amit, *Food Chem. Toxicol.*, 2007, **45**, 1928.
- 30 D. Chanda, K. Shanker, A. Pal, S. Luqman, D. U. Bawankule, D. N. Mani and M. P. Darokar, *J. Toxicol. Sci.*, 2008, **34**, 99.